Theory of (antimicrobial) relativity: When competitors determine a species' drug sensitivity.

Carlos Reding[1*]

[1]*Department of Genetics, School of Medicine, Stanford University. Stanford, CA 94304.*
[*]**Corresponding author:** reding@stanford.edu

The use of antimicrobials without imposing selection on resistant mutants is conjectured (*1*, *2*) to stop the rise of multi-drug resistance, but proof is still elusive. Here I present experimental evidence, underpinned by a mathematical model, showing that antimicrobial sensitivity can be predictably manipulated to achieve the sustained drug efficacy expected from evolution-proof therapies. The model relies on neighbouring microbial species often found in polymicrobial environments. The neighbours can act as drug or carbon sink depending on their drug sensitivity, changing the relative abundance of drug molecules within a focal species and influencing its sensitivity to antimicrobials. Aided by this theory, I doubled the sensitivity of *Escherichia coli* MC4100 to tetracycline in 24h sensitivity tests. Importantly, the effect was maintained after 168h of serial passages akin to those used in evolutionary biology (*3*). My results show that evolutionary-proof therapy design is, indeed, possible. My theory provides a framework to design synthetic neighbours that maximise drug efficacy, while minimising selection on resistance, opening a new venue in drug therapy design.

I. Introduction

Pure cultures are fundamental in microbiology. They consist of one purified microbial species, isolated, for example, to quantify antimicrobial sensitivity (*4*–*6*). Indeed, routine clinical protocols across the globe (*7*, *8*) rely on pure cultures. However, therapies designed using pure cultures target pathogens thriving in polymicrobial environments (*9*). And there, their sensitivity is unpredictable: Pathogens known to be sensitive to an antimicrobial can be interpreted as resistant, and *vice versa*, when the sample contains multiple microbial species (*10*–*12*). Not surprisingly, therapies targeting pathogens in polymicrobial conditions can often fail (*13*). But the underlying mechanism is unknown. Interestingly, the sensitivity of cancers to chemotherapies is also affected by neighbouring microorganisms, particularly those growing within the tumour's microenvironment (*14*, *15*). Here the mechanism is also unknown.

Below I show a simple mathematical model suggesting that neighbouring microorganisms act as carbon or antimicrobial sink and, therefore, change the drug sensitivity of other species (i.e. a pathogen or tumour). The change is predictable, and I used the model to increase two-fold the sensitivity of *Escherichia coli* to tetracycline. Perhaps more importantly, I also show that *E. coli* remained hyper-sensitive to the drug for more than 80 generations—resembling the conjecture outcome of evolution-proof therapies. Moreover, the model can predict the likelihood of drug-tolerance of a pathogen, or a tumour, based on the sensitivity of their neighbouring microorganisms.

II. Results

Drug sensitivity of a focal species is determined by susceptibility of its neighbouring species. Consider j phenotypically distinct species competing for a limited resource, C, and exposed to a drug, A,

cast as the following model:

$$\dot{S}_j = \overbrace{G_j(C)S_j}^{\text{Growth}} \cdot \overbrace{I_j(A)}^{\text{Inhibition}}, \tag{1a}$$

$$\dot{A}_j = \overbrace{-dA_j}^{\text{Decay}} + \overbrace{\varphi_j(A_e - A_j)S_j}^{\text{Fick's Diffusion}}, \tag{1b}$$

$$\dot{A}_e = -dA_e - \sum_{j=1}^{i} \varphi_j(A_e - A_j)S_j \tag{1c}$$

$$\dot{C} = -\sum_{j=1}^{i} \overbrace{U_j(C)S_j}^{\text{C-Uptake}}, \tag{1d}$$

Here, $\dot{S}_j$ and $\dot{A}_j$ represent the density of individuals per unit volume from species j and their content of drug A over time, respectively. $U_j(C)$, the uptake rate of resource C—supplied at concentration C_0—of individuals from species j, is a saturating Monod function proportional to the maximal uptake rate,

$$U_j(C) := \bar{\mu}_j \frac{C}{K_j + C}, \tag{2}$$

where K_j is the half-saturation parameter and the affinity of individuals from species j for the limited resource C is given by $1/K_j$. Their growth rate (i.e. absolute fitness) at a given resource concentration is denoted by $G_j(C) := U_j(C) \cdot y_j$, where y_j is the biomass yield per unit of resource in individuals from species j. Their growth inhibition, by drug A, is described qualitatively by the inhibition function (*16*)

$$I_j(A) := \frac{1}{1 + (A_j/\kappa_j)^{\alpha}}, \text{ where } 0 \leq I_j(A) \leq 1. \tag{3}$$

This function is dimensionless and has two parameters. First, the Hill coefficient α which characterises the cooperativity of the inhibition. And second, κ_j is the affinity of drug A for its target and it can be derived from the drug concentration required to halve the maximal growth rate, so that $A_{50} = 1/\kappa_j$ (*16*). Drug A is supplied at concentration A_0, outside any individuals, at $t = 0$ (so, $A_e(0) = A_0$). The drug then diffuses into individuals from species j with a diffusion coefficient noted by φ_j, and part of A is lost to chemical stability (*17*) at a rate d.

For my first computation I set the number of species $j = 2$, to facilitate later experimental validation, where $I_1(A) = I_2(A)$ and $G_1(C) = G_2(C)$. Thus, individuals from both species are sensitive to A and phenotypically identical. Given Equation 3, the density of individuals from either species as pure cultures declines with higher drug concentrations consistently with standard clinical protocols (*7, 8*) (Figure 1A). To allow experimental validation, I calculated the concentration of A inhibiting the growth of the pure cultures by 90% (IC_{90}) as commonly used in clinic laboratories (*18–20*). The drug sensitivity of each species depends on the values for the parameters $K, \bar{\mu}$, and y of Equation 2 (Figure 1B–D, grey), with values that increase the density of individuals resulting in higher IC_{90}. This is consistent with the *inoculum effect* (*21*), whereby sensitivity tests using larger inocula also report higher minimum inhibitory concentrations.

This phenomenon is exacerbated if both species grow in mixed culture conditions, where both become phenotypically more tolerant to drug A (Figure 1B–D, black). If I were to target, say, individuals from species

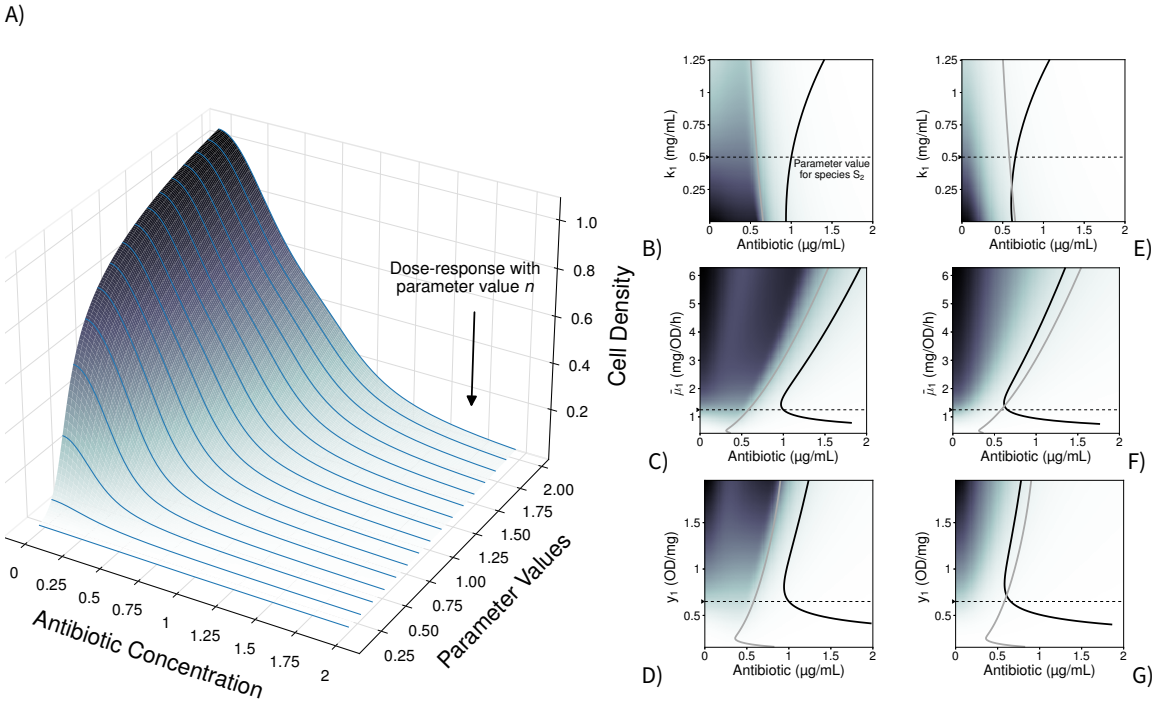

Figure 1. S_1 drug sensitivity profiles in pure and mixed culture growth conditions alongside accessory species S_2. A) Growth of species S_1, with different parameter values (k_1, $\bar{\mu}_1$, and y_1), after 24h of growth in the presence of different antibiotic concentrations. I aggregated the resulting dose-response profiles (blue) to create a density map from low predicted cell density (white) to high predicted cell density (black). **B–D)** IC_{90}, antibiotic concentration inhibiting 90% (IC_{90}) the growth predicted without drug, resulting with different parameters values for the half-saturation parameter k_1 (B), maximal carbon up-take $\bar{\mu}_1$ (C), or biomass yield y_s (D) in equation 1 when species S_2 is drug-sensitive. The IC_{90} for species S_1 growing as pure cultures is shown in grey, and growing in mixed culture with S_2 are shown in black. The parameter values for species S_2 were fixed at a value noted by a black arrow on the y-axis, followed by a dotted black line. **E–G)** Change in IC_{90}, as in Figures B–C), when the competing species S_2 is *not* drug-sensitive.

S_1, doing so when the species is surrounded by S_2 would require more drug. This is the case of pancreatic ductal adenocarcinoma with bacteria growing in its microenvironment (*14*). More generally, genotypes analog to S_1 should increase their drug tolerance when they are surrounded by similarly sensitive species.

To test this hypothesis, I mixed equal proportions of *Escherichia coli* Wyl and *Salmonella typhimurium* SL1344 in minimal media supplemented with different concentrations of tetracycline (see Methods). Both species have similar sensitivity to this antibiotic, 0.232±0.003 and 0.276±0.016 μg/mL of tetracycline (mean IC_{90} ± 95% confidence, with $n = 8$ replicates, see Methods). This approximates to $I_1(A) \approx I_2(A)$, as laid out by the theory above. The chromosome of *E. coli* Wyl carries *yfp*, gene encoding a yellow fluorescence protein (YFP), so I tracked its density in mixed culture conditions. Consistently with Equations 1a–d, the bacterium was around 23% more tolerant to tetracycline when it grew in mixed culture with *S. typhimurium* (Mann-Whitney U-test $p = 1.554 \times 10^{-4}, ranksum = 36$ with $n = 8$ replicates, Figure 2A).

Next, I explored in the model the case where individuals from both species have different sensitivities to drug A ($I_1(A) \neq I_2(A)$). This scenario is akin to pathogens such as *C. difficile* growing alongside human cells (*22*) where the latter are unaffected by the drug ($I_2(A) \approx 1$). The model now predicts a subset of values for K, y, and $\bar{\mu}$ that make S_1 *more* sensitive to the drug in the presence of individuals from species S_2 (Figure 1E–G). To test this prediction, I mixed equal proportions of two constructs of *Escherichia coli* with

different sensitivities to tetracycline. One construct is Wyl, used above, who is sensitive to the antibiotic. The other construct is GB(c), harbouring a non-transmissible plasmid carrying the gene *tet(36)* (*23*) and, therefore, resistant to the drug. Tetracycline binds to the bacterial ribosome, inhibiting protein synthesis (*24*), and *tet(36)* provides ribosomal protection against tetracycline (*23*) without degrading the antibiotic. The IC_{90} for this construct was 6.106 ± 0.272 μg/mL of tetracycline (mean IC_{90} ± 90% confidence with $n = 8$ replicates). Now, $I_1(A) \ll I_2(A)$ satisfies the assumption above. The IC_{90} for *E. coli* Wyl was 0.232 ± 0.003 μg/mL of tetracycline as pure culture. Growing alongside drug-resistant GB(c), however, it was 0.112 ± 0.003 μg/mL (Figure 2B).

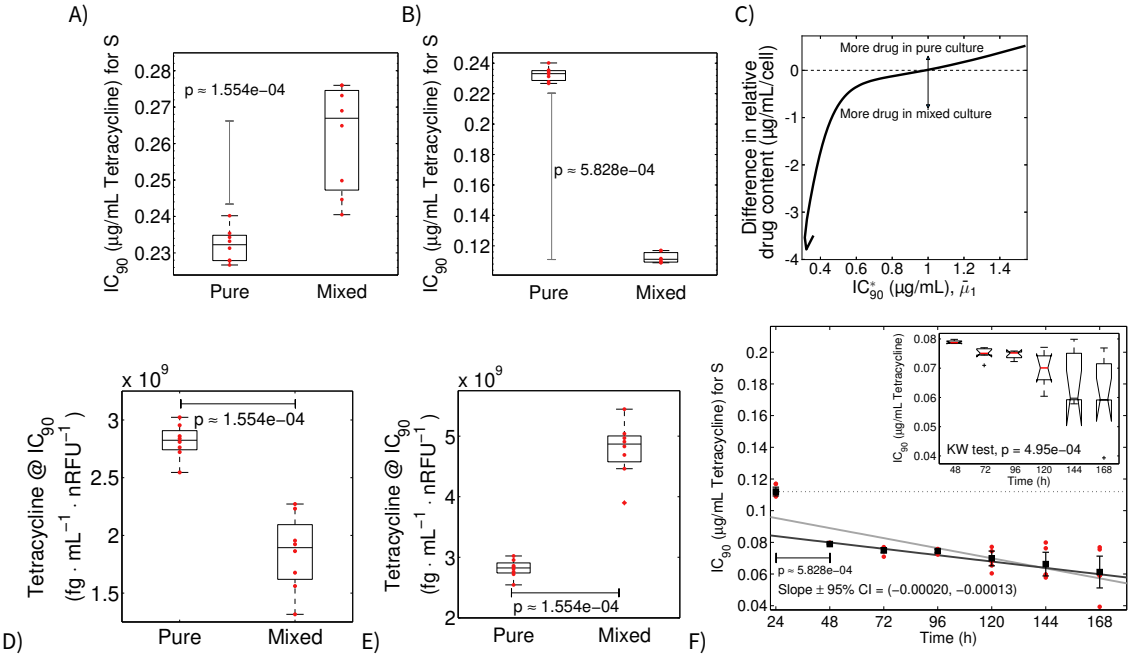

Figure 2. Changes in IC_{90} of drug-sensitive *Escherichia coli* Wyl are consistent with theoretical predictions. A–B) IC_{90} for tetracycline of *Escherichia coli* Wyl in pure culture, and in mixed culture with *Salmonella typhimurium* (A) and *Escherichia coli* GB(c) (B). The IC_{90} for *S. typhimurium* in pure culture was 0.276 ± 0.016 μg/mL of tetracycline (mean ± 95% confidence), and 6.106 ± 0.272 μg/mL for *E. coli* GB(c). The box plot shows the median (centre of the box), 25th, and 75th percentile of the dataset. The whiskers extend to the most extreme data points that are not outliers, which are individually represented. Raw data is represented as red dots. The *p* value shown corresponds to a Mann-Whitney U-test. **C)** Theoretical difference in relative drug content—antibiotic molecules per cell–of S_1 between pure culture conditions, and mixed culture with *drug-sensitive* S_2 for different $\bar{\mu}$ values (for all parameters in Figure S1). Positive values denote higher content of antibiotic per cell in pure culture conditions, whereas negative values denote higher antibiotic per cell in mixed culture. Lack of difference is represented by a horizontal, dotted line. **D–E)** Estimation of tetracycline content from experimental data of *E. coli* Wyl growing alongside *Salmonella typhimurium* (D) and *E. coli* GB(c) (E). The box plots show the median (centre of the box), 25th, and 75th percentile of the dataset. The whiskers extend to the most extreme data points that are not outliers, which are individually represented. Raw data is represented as red dots. The *p* value shown corresponds to a Mann-Whitney U-test. **F)** Variation in IC_{90} of *E. coli* Wyl in mixed culture over time. The errorbars denote mean IC_{90} and 95% confidence, and raw data is shown as red dots. The *p* value shown corresponds to a Mann-Whitney U-test. I fitted a linear model to IC_{90} data including (grey) and excluding the IC_{90} at 24h, and showed the slope parameter of the case with the lowest *p*. The inset show the *p* value of a Kruskal Wallis one-way ANOVA applied to IC_{90} data excluding that measured at 24h. The box plot shows the median in red, 25th, and 75th percentile of the dataset. The whiskers extend to the most extreme data points that are not outliers, which are individually represented as a black cross.

Neighbouring species S_2 determines drug availability for S_1. Above I noted that parameter values leading to higher density of individuals in pure culture, also led to higher IC_{90}. When $I_1(A) \approx I_2(A)$, Equations 1a–d suggest that individuals from one species change the drug availability, measured as relative drug molecules per individual, for the other. Thus, when species S_2 absorbs its share of drug in mixed culture conditions, there is less of it available for species S_1 resulting in less drug per individual (Figure S1A–C)—and *vice versa*. However, when $I_1(A) \neq I_2(A)$, the least sensitive species barely absorbs drug. The change in drug availability occurs through a different mechanism. The least sensitive species is able to remove a higher share of the limited resource, C, as its growth is unaffected by the drug. Thus, the growth of the most sensitive species is limited (*25*), leaving more drug per individual of this species (Figure S1D–F).

To verify this rationale, I estimated the content of tetracycline in *E. coli* Wyl by dividing the bacterium's culture density, measured in relative fluorescence units to allow tracking in mixed culture conditions, by the concentration of tetracycline defining its IC_{90}. The estimates resemble closely the theoretical predictions in Figure 2C: *E. coli* Wyl contains approximately 20% less tetracycline growing next to *Salmonella typhimurium* (Figure 2D) and 65% more tetracycline growing alongside drug-resistant GB(c) (Figures 2E).

Now, experiments of parallel evolution show that *acr*, operon responsible for the multi-drug efflux pump AcrAB-TolC (*26*), undergoes genomic amplification in *E. coli* MC4100 (*3*). Thus, MC4100 overcomes the exposure to doxycycline, a type of tetracycline drug, within five days given its increased capacity to remove antibiotic molecules (*3*). Other strains of *E. coli* show identical adaptation (*27*). To test whether Wyl, MC4100 derivative sensitive to tetracycline, overcomes its exposure to the drug I propagated a culture containing equal proportions of *E. coli* Wyl and GB(c) for 168h. If Wyl acquires a mutation, such as the amplification of *acr*, that protects it against tetracycline I would expect greater IC_{90} over time. However, as Figure 2F illustrates, the IC_{90} of Wyl was further reduced during this period.

III. Discussion

My theory reconciles conflictive sensitivity data reported through direct sensitivity tests (*7, 10, 11*)—drug sensitivity tests that skip the isolation and purification of a pathogen (*28*–*30*). Using direct testing, pathogens known to be sensitive to a drug can be interpreted as resistant and *vice versa* (*10, 31*). While direct testing shortens turnaround time in hospitals, allowing to initiate therapies earlier (*32*), international guidelines (*7*) do not recommend these tests as they can be misleading. A simple mathematical model can explain why such inconsistencies occur.

The predictability of changes in sensitivity in polymicrobial environments poses the following question: Can we exploit the underlying principle? 'Evolution-proof' therapies are the next frontier in the treatment of both infectious diseases (*2*) and cancers (*33*), but whether they exist is still a conjecture. A corollary for the above inconsistencies is that pathogens can have multiple sensitivities to the same drug, and my model and data suggest that the underlying principle could be used to develop strategies that 'sensitise' cancers and pathogens to chemotherapies. Mine is a very simple model inspired by the polymicrobial ecosystem where pathogens thrive, so I do not wish to over state its predictive power. For example, it lacks an immune response or environmental complexities found in the human body. But it shows that evolution-proof strategies are indeed possible. This, however, this does not mean adaptation stops. Data in Figure 2F show adaptation of Wyl, given the change in standard error in IC_{90}. Now, a successful mutant must not only be resistant to the drug, but also fit enough to outcompete its neighbours—with a lower supply of mutants imposed by its neighbour's competitive suppression (*25*).

This work is focused on bacteria as they can easily be grown in a laboratory or labelled. But the model can also apply to cancers. The drug content in pancreatic ductal adenocarcinoma is lower in the tumour when bacteria are present (*14*). My model suggests these bacteria would be acting as drug sink, absorbing part of the drug and causing the tolerance to chemotherapies reported in Ref. Geller *et al.* (*14*).

IV. Methods

Media and Strains. The strains of *Escherichia coli* GB(c) and Wyl (*34*) were a gift from Remy Chait and Roy Kishony, and *Salmonella typhimurium* SL1344 (*35*) a gift from Markus Arnoldini and Martin Ackermann. Experiments were conducted in M9 minimal media supplemented with 0.4% glucose and 0.1% casamino acids and supplemented with tetracycline. I made tetracycline stock solutions from powder stock (Duchefa #0150.0025) at 5mg/mL in deionised water. Subsequent dilutions were made from this stock and kept at 4^oC.

Sensitivity assay. I inoculated a 96-well microtitre plate, containing 150µg/mL of media supplemented with 0–0.5 µg/mL of tetracycline (for *E. coli* Wyl and *S. typhimurium*) or 0–15µg/mL (for *E. coli* GB(c)), with an overnight of each strain to measure drug sensitivity in pure cultures. For sensitivity assays of Wyl in mixed culture conditions I inoculated the microtitre plate, containing 150µg/mL of media supplemented with 0–0.5 µg/mL of tetracycline, with equal proportions of two overnight cultures: Wyl + GB(c) or Wyl + *S. typhimurium*.

I incubated the microtitre plate at 30^oC in a commercial spectrophotometer and measured the optical density of each well at 600nm (OD_{600}), yellow florescence for Wyl (YFP excitation at 505nm, emission at 540nm), and cyan fluorescence for GB(c) (CFP at 430nm/480nm) every 20min for 24h. I defined the minimum inhibitory concentration as the tetracycline concentration able to inhibit 90% of the growth observed in the absence of antibiotic after the 24h incubation period.

Culture readings. Fluorescence protein genes were constitutively expressed with an approximately constant fluorescence to optical density ratio (Figure S2). The number of colony forming units (CFU) is positively correlated with optical density measured at 600nm (OD_{600}) (Figure S3). Thus, I normalised fluorescence readings with respect to optical density readings, using the ratio optical density to fluorescence that I in pure culture conditions, to track the relative abundance of Wyl in mixed culture conditions. Time series data set were blank corrected prior to calculating the minimum inhibitory concentration.

Evolutionary dataset. Following the protocol in Reference (*3*) I propagated a mixed culture, growing in a 96-well microtitre plate containing 150µg/mL of media supplemented with 0–0.5 µg/mL of tetracycline, into a new microtitre plate containing fresh media and antibiotic every 24h. Growth data was blank corrected as above, and used to calculate the IC_{90}.

Code availability: A python implementation of equations 1a–d can be found at https://github.com/rc-reding/papers/tree/master/EvolProof_2020 . The parameter values used can be found in Table S1.

Competing interests: The author declares no competing interests.

References

1. Allen, R. C., Popat, R., Diggle, S. P. & Brown, S. P. Targeting virulence: can we make evolution-proof drugs? *Nat. Rev. Microbiol.* **12,** 300–308 (2014).
2. Bell, G. & MacLean, C. The Search for Evolution-ProofAntibiotics. *Trends Microbiol.* (2017).
3. Pena-Miller, R., Laehnemann, D., Jansen, G., *et al.* When the most potent combination of antibiotics selects for the greatest bacterial load: the smile-frown transition. *PLoS Biol.* **11,** e1001540 (2013).
4. Russell, B. M., Udomsangpetch, R., Rieckmann, K. H., *et al.* Simple in vitro assay for determining the sensitivity of Plasmodium vivax isolates from fresh human blood to antimalarials in areas where P. vivax is endemic. *Antimicrob. Agents. Chemother.* **47,** 170–173 (2003).
5. Reinthaler, F., Posch, J, Feierl, G, *et al.* Antibiotic resistance of E. coli in sewage and sludge. *Water Res.* **37,** 1685–1690 (2003).
6. Bennett, J., Dolin, R. & Blaser, M. *Principles and Practice of Infectious Diseases Churchill Livingstone* **v. 1.** ISBN: 9781455748013 (Elsevier - Health Sciences Division, 2014).
7. *Performance Standards for Antimicrobial Susceptibility Testing; Twenty–Second Informational Supplement M100–S22* 3. Clinical and Laboratory Standards Institute (2012). ISBN: 1-56238-786-3.
8. *Antimicrobials susceptibility testing version 5.0* European Committee on Antimicrobial Susceptibility Testing (European Committee on Antimicrobial Susceptibility Testing, Jan. 2015).
9. Hibbing, M. E., Fuqua, C., Parsek, M. R. & Peterson, S. B. Bacterial competition: surviving and thriving in the microbial jungle. *Nat. Revs. Microbiol.* **8,** 15–25 (2010).
10. Shahidi, A. & Ellner, P. D. Effect of mixed cultures on antibiotic susceptibility testing. *Appl. Microbiol.* **18,** 766–770 (1969).
11. Ellner, P. D. & Johnson, E. Unreliability of Direct Antibiotic Susceptibility Testing on Wound Exudates. *Antimicrob. Agents. Chemother.* **9,** 355–356 (1976).
12. Riedele, C. & Reichl, U. Interspecies effects in a ceftazidime-treated mixed culture of Pseudomonas aeruginosa, Burkholderia cepacia and Staphylococcus aureus: analysis at the single-species level. *J. Antimicrob. Chemother.* **66,** 138–145 (2011).
13. Simón-Soro, A. & Mira, A. Solving the etiology of dental caries. *Trends Microbiol.* **23,** 76–82 (2015).
14. Geller, L. T., Barzily-Rokni, M., Danino, T., *et al.* Potential role of intratumor bacteria in mediating tumor resistance to the chemotherapeutic drug gemcitabine. *Science* **357,** 1156–1160 (2017).
15. Sedighi, M., Zahedi Bialvaei, A., Hamblin, M. R., *et al.* Therapeutic bacteria to combat cancer; current advances, challenges, and opportunities. *Cancer Med.* **8,** 3167–3181 (2019).
16. Klumpp, S., Zhang, Z. & Hwa, T. Growth rate-dependent global effects on gene expression in bacteria. *Cell* **139,** 1366–1375 (2009).
17. Gómez-Pacheco, C., Sánchez-Polo, M, Rivera-Utrilla, J & López-Peñalver, J. Tetracycline degradation in aqueous phase by ultraviolet radiation. *Chem. Eng. J.* **187,** 89–95 (2012).
18. Cedillo-Rivera, R & Munoz, O. In-vitro susceptibility of Giardia lamblia to albendazole, mebendazole and other chemotherapeutic agents. *J. Med. Microbiol.* **37,** 221–224 (1992).

19. Cottrell, M. L., Hadzic, T. & Kashuba, A. D. Clinical pharmacokinetic, pharmacodynamic and drug-interaction profile of the integrase inhibitor dolutegravir. *Clin. Pharmacokinet.* **52,** 981–994 (2013).

20. Baumgartner, M., Bayer, F., Pfrunder-Cardozo, K. R., Buckling, A. & Hall, A. R. Resident microbial communities inhibit growth and antibiotic-resistance evolution of Escherichia coli in human gut microbiome samples. *PLoS Biol.* **18,** e3000465 (2020).

21. Eng, R., Smith, S. & Cherubin, C. Inoculum effect of new beta-lactam antibiotics on Pseudomonas aeruginosa. *Antimicrob. Agents. Chemother.* **26,** 42–47 (1984).

22. Burke, K. E. & Lamont, J. T. Fecal Transplantation for Recurrent Clostridium difficile Infection in Older Adults: A Review. *J. Am. Geriatr. Soc.* **61,** 1394–1398 (2013).

23. Whittle, G, Whitehead, T. R., Hamburger, N, Shoemaker, N. B., Cotta, M. A., *et al.* Identification of a new ribosomal protection type of tetracycline resistance gene, tet(36), from swine manure pits. *Appl. Environ. Microbiol.* **64,** 4151–4158 (2003).

24. Epe, B & Woolley, P. The binding of 6-demethylchlortetracycline to 70S, 50S and 30S ribosomal particles: a quantitative study by fluorescence anisotropy. *EMBO J.* **3,** 121–126 (1984).

25. Day, T., Huijben, S. & Read, A. F. Is selection relevant in the evolutionary emergence of drug resistance? *Trends Microbiol.* **23,** 126–133 (2015).

26. Okusu, H., Ma, D. & Nikaido, H. AcrAB efflux pump plays a major role in the antibiotic resistance phenotype of Escherichia coli multiple-antibiotic-resistance (Mar) mutants. *J. Bacteriol.* **178,** 306–308 (1996).

27. Ayari, Jessica, P., Fabio, G., *et al.* Using a Sequential Regimen to Eliminate Bacteria at Sublethal Antibiotic Dosages. *PLoS Biol.* **13,** e1002104 (Apr. 2015).

28. Serisier, D. J., Jones, G., Tuck, A., Connett, G. & Carroll, M. P. Clinical application of direct sputum sensitivity testing in a severe infective exacerbation of cystic fibrosis. *Pediatr. Pulmonol.* **35,** 463–466 (2003).

29. Jabeen, K., Kumar, H., Farooqi, J., *et al.* Agreement of direct antifungal susceptibility testing from positive blood culture bottles with the conventional method for Candida species. *J. Clin. Microbiol.* **54,** 343–348 (2016).

30. Qamar, F. N., Yousafzai, M. T., Khalid, M., *et al.* Outbreak investigation of ceftriaxone-resistant Salmonella enterica serotype Typhi and its risk factors among the general population in Hyderabad, Pakistan: a matched case-control study. *Lancet Infect. Dis.* **18,** 1368–1376 (2018).

31. Ellis, L. Criminal behavior and r/k selection: An extension of gene-based evolutionary theory. *Deviant Behav* **8,** 149–176 (1987).

32. Coorevits, L., Boelens, J. & Claeys, G. Direct susceptibility testing by disk diffusion on clinical samples: a rapid and accurate tool for antibiotic stewardship. *Eur. J. Clin. Microbiol. Infect. Dis.* **34,** 1207–1212 (2015).

33. Archetti, M. & Pienta, K. J. Cooperation among cancer cells: applying game theory to cancer. *Nat. Rev. Cancer* **19,** 110–117 (2019).

34. Chait, R., Craney, A & Kishony, R. Antibiotic interactions that select against resistance. *Nature* **446,** 668–671 (2007).

281 *35.* Arnoldini, M., Vizcarra, I. A., Peña-Miller, R., *et al.* Bistable expression of virulence genes in salmonella
282 leads to the formation of an antibiotic-tolerant subpopulation. *PLoS Biol.* **12,** e1001928 (2014).

V. Supplementary Tables

Table S1. Model parameters for Equations 1a–d, 2 and 3.

Parameter	Description	Value
$\bar{\mu}_j$	Maximal carbon uptake rate	1.25 mg / OD / h
K_j	Half-saturation constant	0.5 mg / mL
y_j	Biomass yield	0.65 OD / mg
d	Drug degradation rate	10^{-4} / h
$\varkappa_j$	Affinity of drug A for species type j	0.1 mL / µg
φ_j	Diffusion coefficient	0.1 mm^2 / s
A_0	Initial drug concentration	2 µg / mL
C_0	Initial carbon concentration	2 mg / mL

VI. Supplementary Figures

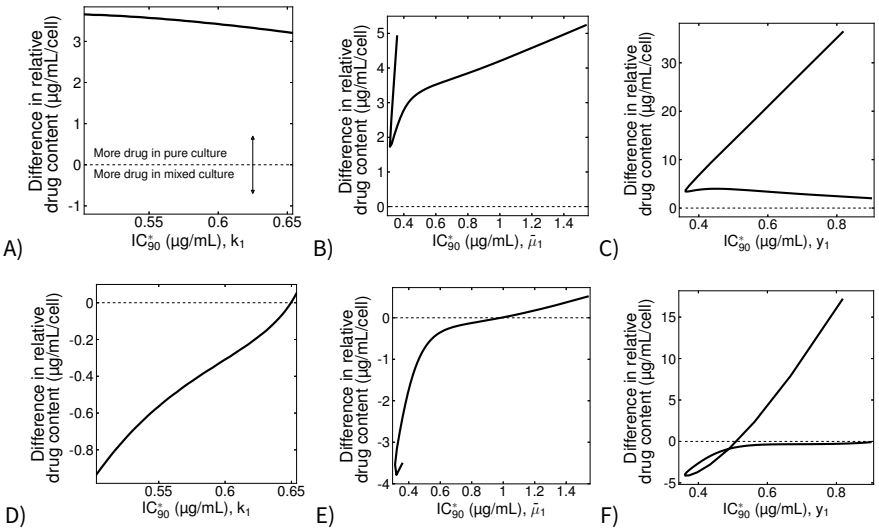

Figure S1. Drug concent in individuals from species S_1 in pure and mixed growth conditions. A–C) Theoretical difference in relative drug content—antibiotic molecules per cell–of S_1 between pure culture conditions, and mixed culture with *drug-sensitive* S_2. A), B) and C) illustrate the prediction when changing the parameter k, $\bar{\mu}$, and y, respectively. The difference is positive (>0) when the relative content of antibiotic is higher in pure culture conditions, whereas is negative (<0) when the content is higher in mixed culture conditions. Lack of difference is represented by a horizontal, dotted line. **D–F)** Theoretical difference in relative drug content—antibiotic molecules per cell–of S_1 between pure culture conditions, and mixed culture with *drug-insensitive* S_2. A), B) and C) illustrate the prediction when changing the parameter k, $\bar{\mu}$, and y, respectively. The difference is positive (>0) when the relative content of antibiotic is higher in pure culture conditions, whereas is negative (<0) when the content is higher in mixed culture conditions. Lack of difference is represented by a horizontal, dotted line.

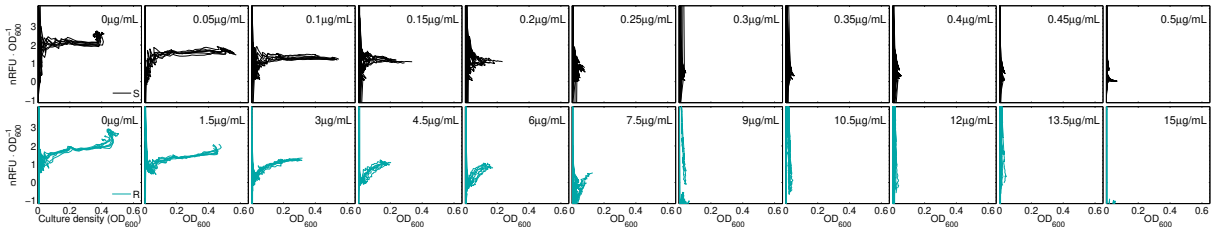

296 **Figure S2. Changes in relative fluorescence over time in both Wyl and GB(c) strains.** Raw change in florescence, per
297 optical density units, measured every 20min for 24h for *E. coli* Wyl (black) and GB(c). Each column represents the data set
298 for each tetracycline concentration used.

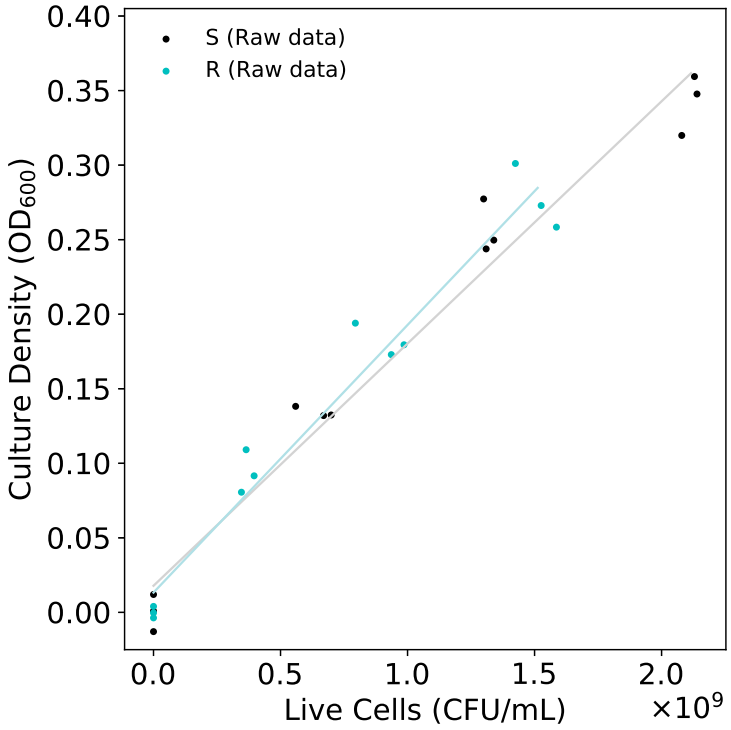

300 **Figure S3. Calibration curve to translate optical density data to number of *Escherichia coli* cells.** I fitted the linear
301 model $a = bx + c$ to optical density and colony counting data (dots) to calculate the number of optical density units
302 (OD_{600}) per cell. a denotes the optical density readings measured at 600nm, c the crossing point with the $y-$axis when
303 $x = 0$, and b the conversion factor between optical density and number of cells (x). I interpolating optical density readings
304 to calculate the number of cells within a culture as $x = (a - c)/b$. For the strain S, $b = 1.62 \times 10^{-10}\ OD \cdot mL \cdot CFU^{-1}$
305 and $c = 1.78 \times 10^{-2}\ OD$, whereas for R $b = 1.79 \times 10^{-10}\ OD \cdot mL \cdot CFU^{-1}$ and $c = 1.33 \times 10^{-2}\ OD$.